DOI: 10.1002/chem.200500562

Controlled Nanozeolite-Assembled Electrode: Remarkable Enzyme-Immobilization Ability and High Sensitivity as Biosensor

Tao Yu, Yahong Zhang,* Chunping You, Jihua Zhuang, Bo Wang, Baohong Liu, Yijin Kang, and Yi Tang*[a]

Abstract: An enzyme-immobilized nanozeolite-assembled electrode was prepared by controlled assembly of nanometer-sized Linder type-L zeolite (nano-LTL-zeolite) on an indium tin oxide (ITO) glass electrode surface, and subsequent immobilization of cytochrome *c*. Cyclic voltammetric (CV) and amperometric experiments showed that, relative to other reported electrodes, the enzyme-immobilized electrodes possess fast electron-transfer rates ($2.2\ s^{-1}$), a broad linear range ($15–540\ \mu mol\ L^{-1}$), a low detection limit ($3.2\ nmol\ L^{-1}$), a remarkably long lifetime (5 months), and high stability in the pH range 5–10. These characteristics could be due to the fact that nanozeolites assembled on ITO have high immobilization ability and facilitate interaction with enzymes. The function controllability of these enzyme electrodes, resulting from the facile manipulability of nanozeolite-assembled layers, may provide a possibility to rationally design biosensors.

Keywords: cyclic voltammetry · enzymes · nanostructures · zeolites

Introduction

Nanoscience is displaying more and more significance for science and technology development. Its development is resulting in great breakthroughs in physics, chemistry, and biology, and has driven many researchers to investigate the possibilities of applying nano-/nanoporous materials to design structural, electromagnetic, optical, and catalytic materials.[1–4] Enzyme-based biosensors is an important research field, as a result of their potential application to a wide range of analytical tasks, such as clinical diagnosis, the food industry, environmental monitoring, and bioassays.[5–6] Many kinds of materials, including biomimetic and inorganic silica,[7–8] clay,[9] zeolites,[10] porous alumina,[11] montmorillonite,[12] hydrogel polymers,[13–14] and self-assembled monolayers[15–17] have been studied as enzyme carriers, by using established strategies for enzyme immobilization.[18–21] Compared with these materials, nanomaterials should have a clear advantage due to the remarkably large surface area available for enzyme immobilization. Therefore, investigations concerned with the attachment of enzymes or other functional proteins onto nanoscale materials are arousing more and more attention, and studies of biosensors involving inorganic nanoparticles,[22–23] pillars,[24] and carbon nanotubes[25] as enzyme-immobilized carriers have been reported. However, due to several challenges concerning the enhancement of the enzyme immobilization, the preservation of enzyme activity, the simplification of the enzyme immobilization process and prolonging the lifetime of the biosensors, investigation of new strategies and materials for enzyme immobilization is still a prevailing subject in the design of biosensors.

It is known that the performance of nanomaterials in any application is strongly dependent upon their physicochemical characteristics and their interactions with the guest species. Besides their large surface area, suitable interaction of the nanoparticles with the guest species is another crucial factor. A weak interaction could lead to a weak immobilization of guests, while an excessive interaction could cause the loss of enzyme activity. Compared with other immobilization methods, physical adsorption plays an important role when immobilizing enzymes, because of the more gentle immobilization conditions, with respect to the techniques of matrix embedding, cast film entrapment, and covalent attachment.[26] However, the resulting low level of enzyme immobilization limits its application. Zeolite nanoparticles (nanozeolite), which displayed good interaction with bio-

[a] T. Yu, Dr. Y. Zhang, C. You, J. Zhuang, B. Wang, Prof. B. Liu, Y. Kang, Prof. Y. Tang
Department of Chemistry and
Shanghai Key Laboratory of Molecular Catalysis and Innovative Materials
Fudan University, 200433 (China)
Fax: (+8621) 6564-1740
E-mail: zhangyh@fudan.edu.cn
yitang@fudan.edu.cn

molecules in our previous work[27] possess excellent characteristics, such as a large clean surface (i.e., without any protection or surface-modifying agent, as in the case of metal nanoparticles[28]), plentiful and tunable surface properties (e.g., adjustable surface charge and hydrophilicity/hydrophobicity), and high dispersibility in both aqueous and organic solutions[29] (which is different from previously reported materials with poor solubility, e.g., carbon nanotubes[30]). These characteristics gives them a very high adsorption capability and a facile self-assembly character,[31] making them promising candidates for the immobilization of enzymes and the construction of enzyme electrodes.

In this paper, we report on the successful construction of a series of enzyme electrodes, named as Cyto-*c*/nano-LTL-zeolite/ITO, with controllable levels of enzyme immobilization, by assembling nanometer-sized Linder type-L zeolite (nano-LTL-zeolite) on indium tin oxide (ITO) glass electrode surfaces, by means of a layer-by-layer (LbL) technique. Cytochrome *c* (Cyto-*c*), which is a model protein, is then adsorbed; it is a very important electron carrier for electron transfer in vivo and in vitro[32,33]. It was found that the Cyto-*c*/nano-LTL-zeolite/ITO electrode possessed a large capacity for enzyme immobilization and provided a suitable interaction with Cyto-*c*, thus leading to direct and good electron-transfer behavior. Fast-response times, a broad linear range, long-lived stability and a low detection limit were found when it was applied as a biosensor to detect hydrogen peroxide. Moreover, the electron-transfer behavior and biocatalytic property of the enzyme electrode could be facilely controlled by adjusting the thickness of the nanozeolite films, thus regulating the amount of the immobilized enzyme, with good electrochemical and biocatalytic activity. This behavior could open up a possibility for the rational design of enzyme electrodes with different requirements.

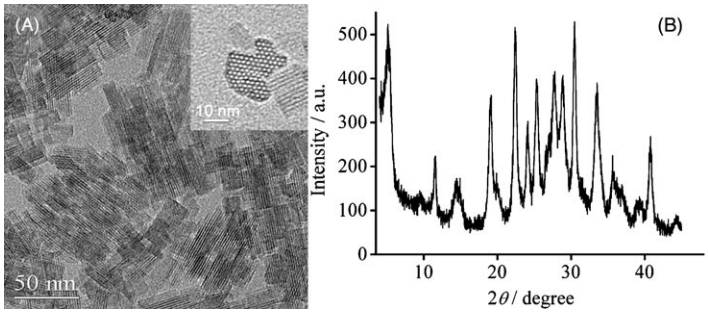

Figure 1. A) A TEM image of nano-LTL-zeolites and their 1D microporous structure (inset); B) XRD pattern of the nano-LTL-zeolites.

Results

Construction of the nanozeolite enzyme electrodes: The Cyto-*c*/nano-LTL-zeolite/ITO electrode was constructed by assembling the nano-LTL-zeolite on the ITO electrode with layer-by-layer (LbL) technology,[34] and then immersing the nanozeolite-assembled electrode in Cyto-*c* ($0.3\,mg\,mL^{-1}$) phosphate buffer solution ($20\,mmol\,L^{-1}$, pH 7) at 277 K overnight. The nano-LTL-zeolite used was a kind of alumino-silicate crystal with 1D 12-membered ring micropores (ca. 0.71 nm in diameter);[35] its morphology and crystalline type are shown in Figure 1. The transmission electron microscopy (TEM) images at high resolution clearly identify the micropore opening array (Figure 1A, inset) and the nanometer-sized (40×80 nm) spindly morphology (Figure 1A). The X-ray diffraction (XRD) pattern confirms the LTL crystal structure (Figure 1B). Figure 2 displays the surface morphologies of the electrodes with different LTL-nanozeolite assembled layers. Evidently, the density and uniformity of the assembled layers on the electrodes increase with the number of nanozeolite-assembling cycles. The LbL assembly process of producing nanozeolites avoided the use of a matrix (e.g., carbon paste), as is the case when fabricating conventional zeolite-modified electrodes,[10b] and may increase the effective contact area of the nanozeolite to both enzyme molecules and the ITO electrode. More importantly, according to our experimental data,[36] the amount of Cyto-*c* immobilized on the Cyto-*c*/nano-LTL-zeolite/ITO electrode reached 37, 57, and $66\,\mu g\,cm^{-2}$ with 3, 5, and 7 nanozeolite assembled layers, respectively. This method provides a possibility to control the amount of immobilized Cyto-*c* by changing the amount of nanozeolites being deposited.

Electrochemical behavior of the Cyto-*c*/nano-LTL-zeolite/ITO electrode: Cyclic voltammograms (CV) of a nano-LTL-

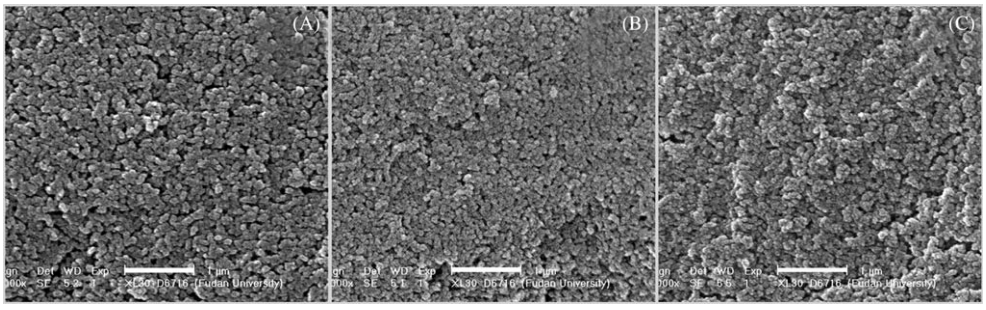

Figure 2. Surface morphologies of nano-LTL-zeolite-assembled electrodes with a different number of nanozeolite-assembled layers: A) 3 layers, B) 5 layers, and C) 7 layers. The scale-bar in each image is 1 μm.

zeolite/ITO electrode with or without immobilized Cyto-*c* were measured in phosphate buffer solution (20 mmol L^{-1}, pH 7) (Figure 3). Two stable redox peaks at +15 and

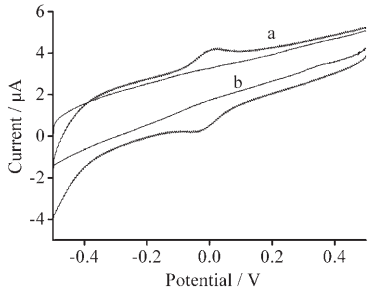

Figure 3. Cyclic voltammograms of Cyto-*c*/nano-LTL-zeolite (5 layers)/ITO electrode, with (a), and without (b) immobilized Cyto-*c*, in phosphate buffer solution (20 mmol L^{-1}, pH 7.0). The scan rate is 60 mV s^{-1}.

−44 mV, at a scan rate of 100 mV s^{-1}, were observed when Cyto-*c* was immobilized on the nanozeolite-assembled electrode, while no electrochemical response was displayed before the Cyto-*c* immobilization process. These results show that a direct electron-transfer process takes place between the immobilized Cyto-*c* and the nanozeolite-assembled electrode,[37] and that the immobilized Cyto-*c* has good electrochemical activity. The half-wave potential $E_{1/2}$ value was estimated to be −18.5 mV, and this negative shift, relative to that of Cyto-*c* in solution (+17 mV vs SCE),[38] could be attributed to the interaction between nano-LTL-zeolite and Cyto-*c*. The electron-transfer rate constant (k_s) was estimated from the Laviron model equation [Eq. (1)][39] as 2.2 s^{-1} ($\alpha = 0.5$), by measuring the peak-to-peak separation

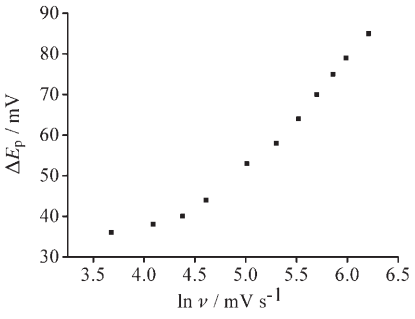

Figure 4. Relationship between the peak-to-peak separation and the scan rate, ν (40–500 mV s^{-1}) of a Cyto-*c*/nano-LTL-zeolite (5 layers)/ITO electrode.

values ΔE_p (Figure 4) of CV curves at different scan rates, ranging from 40 to 500 mV s^{-1}.

$$\Delta E_p = \frac{RT}{n\mathrm{F}\alpha(1-\alpha)}\ln\nu + \frac{RT}{n\mathrm{F}(1-\alpha)}\ln(1-\alpha) + \frac{RT}{nF\alpha}\ln\alpha - \frac{1}{\alpha(1-\alpha)}\ln\left(\frac{RT}{n\mathrm{F}}\right)^{\frac{RT}{nF}} - \frac{RT}{n\mathrm{F}\alpha(1-\alpha)}\ln k_S \quad (1)$$

Interestingly, when the pH value of the system was changed to relatively more acidic or basic conditions, the peak position and ΔE_p value hardly shifted, while a slight decrease of the peak current was observed (Figure 5). These

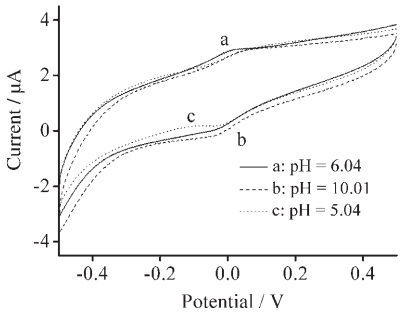

Figure 5. Cyclic voltammograms of a Cyto-*c*/nano-LTL-zeolite (5 layers)/ITO electrode at different pH values: a) 6.04, b) 10.01, and c) 5.04. The scan rate is 60 mV s^{-1}.

results indicate that the electron-transfer process could not be affected by pH-value changes from 5 to 10, and the electrochemical activity of immobilized Cyto-*c* could be maintained over a broad pH-value range. Additionally, the Cyto-*c*/nano-LTL-zeolite/ITO electrode still exhibited an evident electrochemical response after five months storage at 277 K.

Amperometric response of the Cyto-*c*/nano-LTL-zeolite/ITO electrode as a biosensor: The biosensor function of the Cyto-*c*/nano-LTL-zeolite/ITO electrode was evaluated by detecting hydrogen peroxide, since the detection of hydrogen peroxide plays an important role in many fields, including industry, environmental protection, and clinical control.[40–43] Figure 6A shows amperometric catalytic responses of the Cyto-*c*/nano-LTL-zeolite/ITO electrodes after the addition of an aqueous solution of H_2O_2 (60 mmol L^{-1}, 2.5 μL) into phosphate buffer solution (10 mL, 20 mmol L^{-1}, pH 7). The best linear relationship between the response and the H_2O_2 concentration was exhibited in the range 15–540 μmol L^{-1} (Figure 6B), and its apparent Michaelis–Menten constant (K_{app}^{M}[44]), which was calculated by using the Lineweaver–Burk equation [Eq. (2)],[45–46] was within the range 200–300 μmol L^{-1} (Figure 6C).

$$\frac{1}{I_{cat}} = \frac{1}{n\mathrm{F}A\Gamma k_{cat}} + \frac{K_M^{app}}{n\mathrm{F}A\Gamma k_{cat} c_S} \quad (2)$$

The detection limit was estimated to be as low as 3.2 nmol L^{-1}. Besides, the amperometric response of H_2O_2 on the Cyto-*c*/nano-LTL-zeolite/ITO electrode also showed remarkable long-lived stability (the response just decreased by 30% after 5 months) and its biocatalytic activity was well maintained in the pH range 5–10.

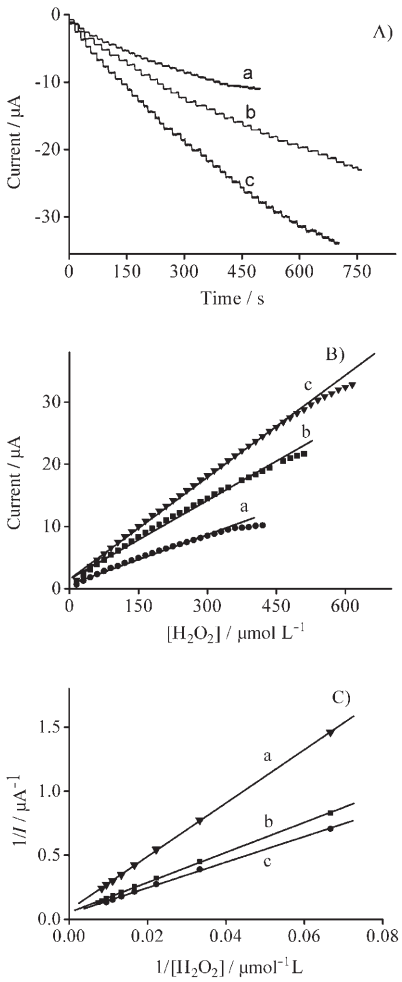

Figure 6. A) Amperometric responses of the Cyto-*c*/nano-LTL-zeolite/ITO electrode at −250 mV upon successive addition of H_2O_2 (60 mmol L^{-1}, 2.5 μL) into a phosphate buffer solution (20 mmol L^{-1}, 10 mL, pH 7); B) calibration curves of the H_2O_2 sensor; C) double-reciprocal plots of the step current to the concentration of H_2O_2. a), b), and c) in the three parts of the figure represent data for electrodes with 3, 5, and 7 nano-LTL-zeolite layers, respectively.

Discussion

As pointed out previously, the Cyto-*c*/nano-LTL-zeolite/ITO electrode displays a clear-cut advantage as a biosensor, due to its electron-transfer behavior and sensor properties. Table 1 displays the function parameters of the Cyto-*c*/nano-LTL-zeolite/ITO electrode prepared in this paper with those of previously reported micrometer-sized zeolites, and some other inorganic nanomaterial-modified enzyme electrodes. It has been found that our electrode presents larger k_s values, a wider linear range, and lower detection limits. These advantages could be attributed to the unique surface property of nanozeolites. Firstly, the nanosized zeolite possesses much larger external surface area (about 58% of its total surface area[47]) than that of micrometer-sized zeolites (generally less than 5% of their total surface area), which would be very beneficial for enzyme molecule adsorption. Moreover, due to their high dispersibility and stability in both aqueous and organic solutions, the surfaces of nanozeolite particles do not need any protective agents to maintain their dimensional stability in the storage and assembly processes, which avoids the probable negative effect during the following enzyme-adsorption step. Figure 7A exhibits the amount of LTL-nanozeolite particles adsorbed per Cyto-*c* moiety at different pH values. The LTL nanozeolites possess not only a very high level of adsorbed enzyme (450–600 mg g^{-1}), but also a wide and stable adsorption range for Cyto-*c* (pH 4–11), which could be an essential prerequisite for constructing

Table 1. Comparison of the parameters of electrochemical and H_2O_2 sensor properties of Cyto-*c*-immobilized electrodes using different enzyme-immobilized inorganic materials. All the Cyto-*c*-immobilized electrodes reported in the table possess a driect electron-transfer processes.

Electrode	k_s [s^{-1}]	K_{app}^{M} [μmol L^{-1}]	Linear range [μmol L^{-1}]	Detection limit [μmol L^{-1}]
Cyto-*c*/nano-LTL-zeolite/ITO[a]	2.2	200	15–540	0.0032
Cyto-*c*/NaY/ITO[48]	0.78	–	8–128	0.32
Cyto-*c*/Multi-walled carbon-nanotube/GC[49]	4.0	857	2–420	–
Cyto-*c*/Gold-colloid/Carbon Paste[50]	1.2	2280[b]	10–1000	–

[a] The Cyto-*c*/nano-LTL-zeolite/ITO electrode contains seven nano-LTL-zeolite assembled layers. [b] The exact data in the reference is 2.28 ± 0.17 mM.

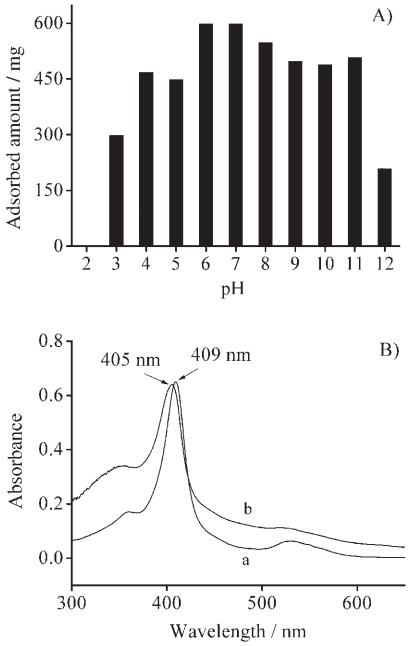

Figure 7. A) The adsorbed amount of LTL-nanozeolite for Cyto-*c* moiety at different pH values; B) UV/visible absorption spectra of Cyto-*c* (0.3 mg mL^{-1}) in a phosphate-buffer solution (20 mmol L^{-1}, pH 7) (a), and a phosphate-buffer solution (20 mmol L^{-1}, pH 7), containing Cyto-*c* (0.3 mg mL^{-1}) and nano-LTL-zeolite particles (0.3 mg mL^{-1}) (b).

good biosensors. It is the high enzyme-adsorption amount that makes the Cyto-*c*/nano-LTL-zeolite/ITO electrode display a lower detection limit and wider linear range, relative to previously investigated enzyme electrodes (Table 1).

The nanozeolite particles could adsorb biomolecules by means of compositive interactions, such as electrostatic and hydrophilic/hydrophobic interactions, because of their tunable surface properties (e.g., adjustable surface charge and hydrophilicity/hydrophobicity).[27] Such compositive interactions may induce the biomolecules (enzyme/protein) to retain their original conformation and orientation for electron-transfer[51–53] and biocatalytic reactions. The nano-LTL-zeolite, with a negatively charged surface, would be suitable for the immobilization of Cyto-*c*. The positively charged six or seven lysine residues surrounding its heme crevice, which play an important role in binding interactions and electron transfer with most of its redox partners,[54–57] could help the immobilization of Cyto-*c* on the surface of the zeolite, by means of electrostatic interaction.[58–62] Meanwhile, the surface hydrophilic/hydrophobic character of the nanozeolite could adjust the microenvironment of immobilized Cyto-*c*. A small shift of the absorbance peak of the Soret band in the UV/visible spectra of the Cyto-*c* and nano-LTL-zeolite solution mixture, corresponding to that of Cyto-*c* solution (Figure 7B), shows that the interactions between Cyto-*c* and nanozeolite do not influence fundamental active conformation of immobilized Cyto-*c*.[63] Therefore, the immobilized enzyme displays good biocatalytic function and sensor properties (Table 1). On the other hand, the interactions between nanozeolite and Cyto-*c*, and the broad pH-adsorption range make the immobilized Cyto-*c* stable and firm enough, and consequently induce the Cyto-*c*/nano-LTL-zeolite/ITO electrode to display a very long lifetime, and a wide pH active range.

More importantly, because of the easy-assembly property of the nanozeolite, the thickness of the nanozeolite film on the electrode could be easily controlled by a LbL assembly technique[64–65], to modulate the electron-transfer behavior and biocatalysis properties (Table 2). As shown in Figure 8, the peak current of the CV curves was enhanced with increasing nanozeolite-film layers, while the electron-transfer rate, that is, k_s always stayed around 2. This indicates that the amount of Cyto-*c*, with good electrochemical activity, could be increased correspondingly with the increase in the number of layers; however the electron-transfer behavior of immobilized Cyto-*c* was not affected by the assembly methods. The step current of the amperometric-response curve (Figure 6A) was also enhanced with an increase in the number of the nanozeolite film layers. The diversity of the linear range, detection limit, and the K_{app}^{M} value of different assembled layers (Table 2) implies that the biocatalytic function of the Cyto-*c*/nano-LTL-zeolite/ITO electrode could be facilely regulated through the LbL strategy, according to the demand for different sensor practices.

Table 2. Electrochemical behavior and biosensor function comparison of Cyto-*c*/nano-LTL-zeolite/ITO electrodes with different nanozeolite-assembled layers.

Number of layers	Peak current[a] [μA]	k_s [s^{-1}]	K_{app}^{M} [$\mu mol\,L^{-1}$]	Linear range [$\mu mol\,L^{-1}$]	Detection limit [$\mu mol\,L^{-1}$]
3	0.245	2.0	300	15–360	0.015
5	0.612	2.2	234	15–480	0.0128
7	0.842	2.2	200	15–540	0.0032

[a] The scan rate is 100 $mV\,s^{-1}$.

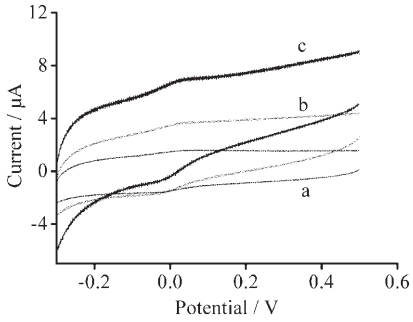

Figure 8. Cyclic voltammograms of Cyto-*c*/nano-LTL-zeolite/ITO electrodes with a) 3, b) 5, and c) 7 nanozeolite-assembled layers in phosphate buffer solution (20 $mmol\,L^{-1}$, pH 7). The scan rate is 100 $mV\,s^{-1}$.

Conclusion

Nano-LTL-zeolite particles were used as enzyme immobilization carriers to construct Cyto-*c*/nano-LTL-zeolite/ITO electrodes by a LbL assembly technique, and their electrochemical and biocatalytic properties were evaluated from CV and amperometric experiments. The results show that the Cyto-*c*/nano-LTL-zeolite/ITO electrodes possess direct electron-transfer behavior, excellent biosensor properties, long lifetimes, and wide pH stability. All the advantages of the Cyto-*c*/nano-LTL-zeolite/ITO electrodes could be contributed to the remarkable enzyme-adsorption ability of nanozeolites, and proper and stable interactions between nanozeolite and Cyto-*c*. In addition, assembling nanozeolites on the electrode by means of LbL technology could control the amount of enzyme immobilized on the Cyto-*c*/nano-LTL-zeolite/ITO electrode, and thus control its biosensor properties by regulating the thickness of the nanozeolite-assembled layers; this makes the rational design of enzyme electrodes possible.

Experimental Section

Apparatus: XRD data was obtained on a Rigaku D/max-IIA diffractometer with $Cu_{K\alpha}$ radiation at 40 kV and 45 mA. Scanning electron microscopy (SEM) was carried out using a Philips XL 30, and TEM studies were performed on a JEOL 200 microscope, with an accelerating voltage of 20 and 200 kV, respectively. Electrochemical experiments were performed at room temperature by using a three-electrode setup, consisting of a saturated calomel reference electrode (SCE), a platinum wire coun-

ter electrode, and an enzyme-immobilized nanozeolite-assembled ITO working electrode. All electrochemical measurements were recorded by using a CHI660A electrochemical working station from CH Instruments, Texas.

Reagents: Fumed silica was obtained from Shanghai Chlorine Alkali Industry. Aluminum foil and potassium hydroxide were obtained from Shanghai Reagent Factory (China). Poly(diallyldimethylammonium chloride) (PDDA, $M_w < 200{,}000$) was obtained from Aldrich. Horse heart Cyto-*c* was purchased from Sigma and used without further purification. A phosphate buffer solution (20 mmol L^{-1}, pH 7) served as the supporting electrolyte. All solutions were prepared with deionized water, purified with a Milli Q plus system.

Synthesis of nano-LTL-zeolite colloids: Nano-LTL-zeolite colloids were synthesized in a clear homogeneous solution with a molar composition of $10\,K_2O{:}1\,Al_2O_3{:}20\,SiO_2{:}400\,H_2O$, according to literature.[66] After stirring overnight, the precursor solution was crystallized in an autoclave at 180 °C for 2 days. The nano-LTL-zeolite colloids obtained were purified by centrifugation and redispersion in highly pure water five times; the last sols were dispersed in highly pure water with a solid content of 1.0 wt %.

Construction of the Cyto-*c*/nano-LTL-zeolite/ITO electrode: The nano-LTL-zeolite assembled ITO electrode was prepared by a LbL technique: Firstly, the ITO electrode was cleaned with acetone and treated in a basic solution ($NH_4OH/H_2O_2/H_2O = 1{:}1{:}5$ volume ratio) to remove impurities on the surface. The electrode was then coated with one-layer polyelectrolyte films of cationic PDDA, which provided a positively charged surface. The negatively charged nanozeolites and PDDA were deposited alternatively on this positively charged surface, to form homogeneous nanozeolite/PDDA multilayers. All of the adsorption steps were performed at ambient temperature for 20 min, and after each adsorption step the electrode was washed with distilled water. Cyto-*c* immobilization was achieved by immersing a 1 cm^2 assembled electrode in a Cyto-*c* (0.3 mg mL^{-1}) phosphate buffer solution (20 mmol L^{-1}, pH 7) at 277 K overnight.

Measurement of the Cyto-*c* adsorption amount on nano-LTL-zeolite surfaces: Adsorption of Cyto-*c* on the nano-LTL-zeolite surface was performed for 1.5 h, by incubation of mixtures of Cyto-*c* (0.1 mg mL^{-1}) and nanozeolite (0.1 mg mL^{-1}) solutions with phosphate buffer solutions (20 mmol L^{-1}, 0.5 mL) of varying pH (2–12). After centrifugal separation, the UV/visible absorption value (280 nm) of supernatant solution was measured to calculate the amounts of Cyto-*c* adsorbed on nanozeolites at different pH values. To calculate the adsorbed amount accurately, a standard curve at $\lambda = 280$ nm was recorded, by using a series of Cyto-*c* solutions of different concentration, with a phosphate buffer solution (20 mmol L^{-1}, pH 7).

CV measurements: CV behavior of the Cyto-*c*/nano-LTL-zeolite/ITO electrodes were studied at different scan rates, from 40 to 500 mV s^{-1}. Prior to the electrochemical measurements buffer solutions were deoxygenated by purging with nitrogen for at least 20 min. To compare results, cyclic voltammetry of a nano-LTL-zeolite/ITO electrode without immobilized Cyto-*c* was also recorded in phosphate buffer solution (20 mmol L^{-1}, pH 7). The CV behavior at different pH values (5–10) and film thicknesses was tested under the same conditions.

Amperometric measurements: The amperometric response of the Cyto-*c*/nano-LTL-zeolite/ITO electrode was measured in a stirred electrochemical glass cell, containing phosphate buffer solution (10 mL, 20 mmol L^{-1}, pH 7). When the electrode had reached a steady state, an aqueous solution of H_2O_2 (60 mmol L^{-1} 2.5 μL) was added to the system and the current response was measured, until there was no current change. The same tests were carried out at different pH values (5–10), and with different numbers of nano-LTL-zeolite assembled layers; the lifetime was also analyzed.

Acknowledgements

The authors greatly appreciate the support of the NSFC (20303003, 20325313, 20473022, 20421303, 20233030) and STCSM (05QMX1403, 05XD14002).

[1] T. G. Schaaff, M. N. Shafigullin, J. T. Khoury, I. Vezmar, R. L. Whetten, W. G. Cullen, P. N. First, C. Gutierrez-Wing, J. Ascensio, M. J. Jose-Yacaman, *J. Phys. Chem. B* **1997**, *101*, 7885.
[2] J. G. Zhao, J. P. O'Daly, R. W. Henkens, J. Stonehuerner, A. L. Crumbliss, *Biosens. Bioelectron.* **1996**, *11*, 493.
[3] R. Elghlebienne, J. J. Storhoff, R. C. Mucic, C. A. Mirkin, *Science* **1997**, *277*, 1078.
[4] J. M. Nam, C. S. Thaxton, C. A. Mirkin, *Science* **2003**, *301*, 1884.
[5] I. Willner, E. Katz, *Angew. Chem.* **2000**, *112*, 1230; *Angew. Chem. Int. Ed.* **2000**, *39*, 1180.
[6] E. Katz, V. Heleg-Shabtai, B. Willner, I. Willner, Bückmann, F. Andreas, *Bioelectrochem. Bioenerg.* **1997**, *42*, 95.
[7] H. R. Luckarift, J. C. Spain, R. R. Naik, M. O. Stone, *Nat. Biotechnol.* **2004**, *22*, 211.
[8] S. E. Létant, B. R. Hart, S. R. Kane, M. Z. Hadi, J. Shields, J. G. Reynolds, *Adv. Mater.* **2004**, *16*, 689.
[9] C. Lei, F. Lisdat, U. Wollenberger, F. W. Scheller, *Electroanalysis* **1999**, *11*, 274.
[10] a) B. Liu, R. Hu, J. Q. Deng, *Anal. Chem.* **1997**, *69*, 2343; b) A. Walcarius, *Anal. Chim. Acta* **1999**, *384*, 1.
[11] O. Ikeda, M. Ohtani, T. Yamaguchi, A. Komura, *Electrochim. Acta* **1998**, *43*, 833.
[12] C. Fan, Y. Zhuang, G. Li, J. Zhu, D. Zhu, *Electroanalysis* **2000**, *12*, 1156.
[13] R. Huang, N. F. Hu, *Biophys. Chem.* **2003**, *104*, 199.
[14] R. Huang, N. F. Hu, *Bioelectrochemistry* **2001**, *54*, 75.
[15] X. Chen, R. Ferrigno, J. Yang, G. M. Whitesides, *Langmuir* **2002**, *18*, 7009.
[16] P. E. Labibinis, C. D. Bain, R. G. Nuzzo, G. M. Whitesides, *J. Phys. Chem.* **1995**, *99*, 7663.
[17] P. Tengvall, I. Lundstrom, B. Liedberg, *Biomaterials* **1998**, *19*, 407.
[18] F. A. Armstrong, A. M. Bond, H. A. O. Hill, B. N. Oliver, I. S. M. Psalti, *J. Am. Chem. Soc.* **1989**, *111*, 9185.
[19] H. Allen, O. Hill, N. I. Hunt, A. Bond, *J. Electroanal. Chem.* **1997**, *436*, 17.
[20] J. M. Sevilla, T. Pineda, A. J. Román, R. Madueño, M. Blázquez, *J. Electroanal. Chem.* **1998**, *451*, 89.
[21] W. Tischer, P. Wedekind, *Top. Curr. Chem.* **1999**, *200*, 95.
[22] W. J. Parak, D. Gerion, T. Pellegrino, D. Zanchet, C. Micheel, S. C. Williams, R. Boudreau, M. A. Le Gros, C. A. Larabell, A. P. Alivisatos, *Nanotechnology* **2003**, *14*, 15.
[23] Z. Li, N. F. Hu, *J. Electroanal. Chem.* **2003**, *558*, 155.
[24] R. Michel, I. Reviakine, D. Sutherland, C. Fokas, G. Csucs, G. Danuser, N. D. Spencer, M. Textor, *Langmuir* **2002**, *18*, 8580.
[25] R. J. Chen, Y. G. Zhan, D. W. Wang, H. J. Dai, *J. Am. Chem. Soc.* **2001**, *123*, 3838.
[26] a) T. Uwe, Bornscheuer, *Angew. Chem.* **2003**, *115*, 3458; *Angew. Chem. Int. Ed.* **2003**, *42*, 3336; b) H. Tang, J. H. Chen, S. H. Yao, L. H. Nie, G. H. Deng, Y. F. Kuang, *Anal. Biochem.* **2004**, *331*, 89.
[27] a) Y. H. Zhang, X. Y. Wang, W. Shan, B. Wu, H. Fan, X. Yu, Y. Tang, P. Y. Yang, *Angew. Chem.* **2005**, *117*, 621; *Angew. Chem. Int. Ed.* **2005**, *44*, 615; b) Y. H. Zhang, X. J. Yu, X. Y. Wang, W. Shan, P. Y. Yang, Y. Tang, *Chem. Commun.* **2004**, 2882; c) F. Xu, Y. J. Wang, X. D. Wang, Y. H. Zhang, Y. Tang, P. Y. Yang, *Adv. Mater.* **2003**, *15*, 1751.
[28] L. B. Justin. , G. W. Claudia, M. Y. Mario, J. Y. Miguel, *Langmuir* **2004**, *20*, 11778.
[29] W. Shan, Y. H. Zhang, W. L. Yang, C. Ke, Z. Gao, Y. E. Ye, Y. Tang, *Microporous Mesoporous Mater.* **2004**, *69*, 35.
[30] H. Tang, J. H. Chen, S. Z. Yao, L. H. Nie, G. H. Deng, Y. F. Kuang, *Anal. Biochem.* **2004**, *331*, 89.

[31] Y. H. Zhang, F. Chen, W. Shan, J. H. Zhuang, A. G. Dong, W. B. Cai, Y. Tang, *Microporous Mesoporous Mater.* **2003**, *65*, 277.
[32] N. Katsumi, W. R. Hardy, G. H. Michael, H. Li, R. S. James, M. Emanuel, F. Kyoko, T. Ryutaro, N. Nobufumi, O. Hiroyuki, H. R. John, H. B. Gray, *J. Phys. Chem. B* **2003**, *107*, 9947.
[33] S. H. Northrup, K. A. Thomasson, C. M. Miller, P. D. Barker, L. D. Eltis, J. G. Guillemette, A. G. Mauk, S. C. Inglis, *Biochemistry* **1993**, *32*, 6613.
[34] G. Decher, *Science* **1997**, *277*, 1232.
[35] C. Baerlocher, W. M. Meier, D. H. Olson, *Atlas of Zeolites Framework Types*, (Eds: C. Baerlocher, W. M. Meier, D. H. Olson), Elsevier, **2001** p. 170.
[36] The amount of Cyto-*c* adsorbed on the Cyto-*c*/nano-LTL-zeolite/ITO electrodes, with 3, 5, and 7 layers of assembled nanozeolites, was determined by measuring weight changes, before and after adsorbing Cyto-*c*, with a quartz balance at room temperature.
[37] To study the contribution of PDDA during the electron-transfer process, the CV and amperometric-response curves of the ITO electrode modified with only a PPDA layer were measured in a cytochrome *c* phosphate buffer solution (0.3 mg mL^{-1}, pH 7). The results showed no CV peak or amperometric response, which implies that the presence of PDDA in the electrode does not assist the electron-transfer step from Cyto-*c*.
[38] F. M. Hawkridge, T. Kuwana, *Anal. Chem.* **1973**, *45*, 1021.
[39] E. Laviron, *J. Electroanal. Chem.* **1979**, *101*, 19.
[40] P. N. Bartlett, P. R. Birkin, J. H. Wang, F. Palmisano, G. D. Benedetto, *Anal. Chem.* **1998**, *70*, 3685.
[41] J. Wang, Y. Lin, L. Chen, *Analyst* **1993**, *118*, 277.
[42] R. M. Sellers, *Analyst* **1980**, *105*, 950.
[43] H. Y. Wang, R. Guan, C. H. Fan, G. X. Zhu, G. X. Li, *Sens. Actuators B* **2002**, *84*, 214.
[44] D. L. Nelson, M. M. Cox, *Lehninger Principles of Biochemistry*, Worth, **2000** p. 262.
[45] A. H. Heering, J. Hirst, F. A. Armstrong, *J. Phys. Chem. B* **1998**, *102*, 6889.
[46] R. A. Kamin, G. S. Wilson, *Anal. Chem.* **1980**, *52*, 1198.
[47] The external surface area of nano-LTL-zeolite was determined by a t-plot method (thickness range: 0.35–0.5 nm), and the result showed that the external surface area of the nano-LTL-zeolite was about 213.08 m^2 g^{-1}, while its micropore area was 152.99 m^2 g^{-1}. To avoid aggregation of the nanozeolite at high temperature, degassing of the sample was carried out at room temperature.
[48] Z. H. Dai, S. Q. Liu, H. G. Ju, *Electrochim. Acta* **2004**, *49*, 2139.
[49] G. C. Zhao, Z. Z. Yin, L. Zhang, X. W. Wei, *Electrochem. Commun.* **2005**, *7*, 256.
[50] H. X. Ju, S. Q. Liu, B. X. Ge, F. Lisdat, F. W. Scheller, *Electroanalysis* **2002**, *14*, 141.
[51] E. E. Ferapontova, *Electroanalysis* **2004**, *16*, 1101.
[52] S. Zhang, G. Wright, Y. Yang, *Biosens. Bioelectron.* **2000**, *15*, 273.
[53] J. M. Brockman, B. P. Nelson, R. M. Corn, *Annu. Rev. Phys. Chem.* **2000**, *51*, 41.
[54] G. Mclendon, *Acc. Chem. Res.* **1988**, *21*, 160.
[55] J. M. Nocek, J. S. Zhou, S. De Forest, S. Priyadarshy, D. N. Beratan, J. N. Onuchic, B. M. Hoffman, *Chem. Rev.* **1996**, *96*, 2459.
[56] D. Flöck, V. Helm, *Proteins: Struct. Funct. Genet.* **2002**, *47*, 75.
[57] Y. J. Zhen, C. Hoganson, G. T. Babcock, S. Ferguson-Miller, *J. Biol. Chem.* **1999**, *274*, 38042.
[58] V. W. Leesch, J. Bujons, A. G. Mauk, B. M. Hoffman, *Biochemistry* **2000**, *39*, 10132.
[59] M. Fedurco, *Coord. Chem. Rev.* **2000**, *209*, 263.
[60] X. X. Chen, F. Rosaria, J. Yang, G. M. Whitesides, *Langmuir* **2002**, *18*, 7009.
[61] H. M. Daniel, H. Peter, *J. Am. Chem. Soc.* **2001**, *123*, 4062.
[62] K. B. Moritz, W. S. Frieder, L. Fred, *Anal. Chem.* **2004**, *76*, 4665.
[63] C. A. Humberto, V. Brenda, V. D. Rafael, *Bioconjugate Chem.* **2002**, *13*, 1336.
[64] K. H. Rhodes, S. A. Davis, F. Caruso, B. J. Zhang, S. Mann, *Chem. Mater.* **2000**, *12*, 2832.
[65] X. D. Wang, W. L. Yang, Y. Tang, Y. J. Wang, S. K. Fu, Z. Gao, *Chem. Commun.* **2000**, *21*, 2161.
[66] T. Michael, L. Mark, O. Tatsuya, E. D. Mark, S. Masayoshi, *Chem. Mater.* **1995**, *7*, 1734.

Received: May 23, 2005
Published online: October 26, 2005

